Journal of Energy and Power Engineering 20 (2026) 15-30
doi: 10.17265/1934-8975/2026.01.002

Novel Tripartite Managed DC-DC Convertor with Kingpin-Acolyte Based Distributed Consonance Control Strategy for Proficient Power Management in DC Microgrid

K. K. Singh Tomar

Executive Engineer, Uttar Pradesh Power Corporation Ltd., Noida 201301, India

Abstract: A micro-grid is a miniature active delivery network that uses DGs (distributed generations) (both green and conventional), energy storage facilities, and loads to run in either grid-connected or islanded modes. More over to decrease the variations in load voltage, power flow fluctuations, and enhanced the control of DC (direct current) connection with different bus voltage in battery storage unit is most complicated in prior studies. Hence in this paper efficiently proposed the Tripartite Managed DC-DC convertor that highly reduces the load voltage variations in micro grid. As a consequence, in terms of load and input voltage differences, it regulates the voltage in a DC micro grid depending on replacing frequency, service ratio, and patch shift between two vigorous connectors. Then the paper introduces the novel kingpin-acolyte based distributed consonance control strategy for ensuring the balanced power flow and enhanced the battery storage unit control. Control can be achieved by active and passive layers of control in this case. The active stage uses a reference-based droop control technique to assign tonnage components to the batteries for voltage power. The passive align uses sequential multi-agent scheme-oriented distributed solidarity for redistributing the DC bus voltage also procure controlled power transpose within these battery energy storage modules. Consequently, the outcome of the proposed work efficiently described the performances of the controller.

Key words: DC microgrid, tripartite DC-DC Converter, battery energy storage, distributed consonance control, kingpin-acolyte strategy, voltage regulation, power sharing, renewable integration.

1. Introduction

Globally, electrical energy consumption is increasing every day, necessitating the need to generate more electricity more efficiently. With rising concerns about the energy crisis, researchers are increasingly drawn to the production of RERs (renewable energy resources). DG (distributed generation) units [1-6] have recently attracted a lot of attention because they are more powerful, stable, and reliable than traditional power systems. As a result, the MG (microgrid) is a highly effective means of combining multiple DGs as well as energy storage systems, both grid-connected and stand-alone. ESDs (energy storage devices) are important in surpassing DC (direct current) MG (microgrid) systems because they compensate for power generation volatility and load demand.

Fans and telecommunication towers have recently been using DC loads [7-8]. PEV (plug-in electric vehicle) vitalizing stations dependent on DC MG have grown in popularity as they improve performance and reduce emissions. The battery controller is in charge of DC bus voltage regulation, SoC (state of charge), as well as power balancing between distributed energy

Corresponding author: K K Singh Tomar, B. Tech (NIT Calicut), M. Tech, Ph.D. (IIT Kanpur), MBA (NTPC School of Business, Noida), Executive Engineer, Uttar Pradesh Power Corporation Ltd., research fields: DC microgrids, smart grids, advanced distribution management systems (ADMS).

resources. With the goal of adjusting DC bus voltage, SoC, as well as power balancing between DERs (distributed energy resources), the battery controller's peak or inferior control layer, is made up of three organized controlling tactics: decentralized, centralized, as well as distributed/hierarchical control. Even if there is no cooperation with local regulators, a decentralized [9] controller will never require any digital control signals from distinct system components. A centralized controller collects data from the essential [10] gadget of an MG through digital communication links. It has a single point of failure, but it has major benefits for system observability as well as controllability. Such framework requires coherent communication and knowledge swap using distributed consensus algorithms, as well as proper teamwork among the units, to improve this purpose.

Voltage drop between various multiple storage systems as well as changing load creates illegitimate power delivery there in aforementioned conventional droop control techniques. The slender contact graphs might be used to provide an updated power dissipation reference-oriented V-P droop regulation to ensure [11] balanced power sharing between the storage devices. All power outputs as well as SoC of BESUs (Battery Energy Storage Units) may be harmonized through miserly data [12] sharing, ESS (Energy Storage System) established allocation consensus integral control. A leaderless consensus control rule is used to maximize load distribution among various distributed generation modules in DC MG scheme. To gain SoC and power level consensus, battery converters [13] used assigned consensus control.

Using a related method for distributed heterogeneous BESUs, a virtual impedance device was suggested for homogenizing the BESUs energy intensity in DC MG. The ultra-capacitor [14] and battery leader reference voltages were controlled using a leader-follower [15] approach, resulting in heterogeneous consensus clutch of an energy storage solution that is hybrid. In miscellaneous consensus control [16] design, BESUs' nominal voltage as well as frequency magnitudes was utilized rather of their frequencies as well as voltage magnitudes.

Based on the superior literature, this paper suggested a distributed cohesive controlling unit for a straightforward DC MG system that takes into account distributed diverse battery units. The machine contains photovoltaic, wind turbine, as well as BESS, interpolation on numerous loads like alternating current, direct current, as well as electric cars. Six buses are clustered together in a ring in the planned scheme. Due to load volatility, power demand is volatile, while PV (Photovoltaic) and wind power supply fluctuates due to environmental factors. As a consequence, the power as well as voltage flow on the standard coupling point varies greatly. Effective DC line voltage management on multiple buses or different BESUs was required so reduce power flow variability with transients upon its DC line voltage during these situations. For revamp voltage as well as power interchange among BESUs, the designed controller employs the leader-follower principle. As a corollary, multiple control [17-19] strategies for stand-alone DC MG systems in the literature use conventional droop control approaches as well as consensus controlling guidelines to address heterogeneous storage units. In this paper, leader-follower-based cooperative control is used to boost the V-P droop control approach through altering the power relationship. Droop loop controlled energy storage units alter its yield power relation depending its neighbor communication using a fragmented communication network. As a result, with a smaller difference of DC bus voltage, all BESUs attain a regulated energy state and also keep balanced power exchange. The leader-follower oriented mutual control system ensures that neither ESU (Energy Storage Unit) runs out of energy permanently through snagging a balanced energy level among them. As a result, the ESUs' maximum power potential may be utilized the regulate DC link voltage.

2. Literature Survey

Sedaghati et al.'s [20] article offers the novel grid-

connected power management and micro-grid control technique, that consists of a hybrid HRES as well as a 3-phase load. HRES system contains of a PV system, a battery storage system, a super capacitor and a SOFC (solid oxide fuel cell). It describes an impenetrable archetypal for every module. PV was primary source of power, while the SC and BSS are known to have a stable and intermittent load demand, respectively, owing to their different power densities. To maximize the system's stability, the SOFC source was chosen to keep the BSS fully powered. All of these systems, which use multiple DC-DC converters, were linked with standard DC bus in parallel. The DC voltage is then converted to AC using a three-phase VSI (voltage source inverter). An adaptive fractional fuzzy sliding mode control approach was presented using VSI oriented HRES systems in order to preserve power balance as well as adequate load-sharing. The controller in the microgrid will reliably and rapidly track the predefined instructions. A sliding surfaces depending upon fractional ordering was premeditated for stable control strategy performance under load variance. Fuzzy sets based on fractional adaptive rules are often used to estimate the undefined parameters in the micro grid correctly.

For Mehrasa et al. [21], along with its capacity to provide higher active, reactive power as well as highly appropriate power performance improvement, multilevel converters are a viable option in micro grid operations. Using two simultaneous PEC9 (9-level Packed E-Cell) inverters, the article uses a grid linked LCL (Inductor-Capacitor-Inductor filter) filtration micro-size. In a feedback control method to accommodate grid stability and unit power factor inverters according to micro grid needs, PEC9 output current D-q reference frame fluctuations with filter voltages are incorporated. The suggested control strategy is tested using the PEC9 output current-based transfer functions for obtaining efficient controlling parameters.

For Wu et al. [22], as a consequence of fossil-oil crises as well as ecological emissions worsen, the only viable energy system transition option is clean renewable energy. The power generation variability of dispersed renewable energy projects, like solar as well as wind, had a significant impact on power plant design and maintenance. A hybrid energy storage system with an accumulator as well as a super capacitor will solve the problems described above. A hybrid energy storage system, a solitary battery as well as super conductive hybrid energy storage subsystem, as well as a hybrid energy supply micro grid system with independence are utilized depending upon its evaluation of the energy storage specifications on the steady-state functioning of the DC micro grid for the battery-super condenser potable water strategy.

Tummuru et al. [23] present a control approach for grid-connected and islanded operation of renewable-interfaced HESS (Hybrid Energy Storage Systems). For successful synchronization/resync of the microgrid system under contingent situations, a subsequent harmonic-oriented locking loop was utilized. The microgrid system is operated and maintained with an efficient algorithm for adaptive power management in these two modes. A detailed analysis of the HESS performance is given for looking into overall efficacy of suggested strategy. Limited signal averaging simulations were likewise created in order for assessing this technique's efficacy. Such method addresses smooth transitioning among different system sub-modes, and also extra features like increased power conservation as well as power distribution across numerous outlets. Modeling as well as empirical studies is used to verify the feasibility of the proposed strategy.

Toghani Holari et al. [24] proposed a control technique for stable operation of a DC/AC hybrid microgrid under unbalanced generation of CD (Conventional Distributed) units, based on a combination of Lyapunov theory and Input-Output Feedback Linearization (IOFL). PV bucking as well as lithium battery-depended bidirectional DC/DC converters provided the DC connections for the proposed hybrid micro grid. The DC connection was linked to a converter DC/AC, which was designed to supply the active as well as reactive power required for

creating the appropriate waveforms for the typical coupling point voltages.

Worku et al. [25] discuss effective power management micro grids regulation with energy storage. Centered on 3 distributed energy infrastructure, named as PV, battery, as well as local active load fuel generators, the proposed control scheme improves the micro grid's reliability and longevity. Microgrid control requires coordination between DERs and energy storage. The RTDS (Real Time Digital Simulator) was used for building machine model as well as control technique. A decoupling d-q current management technique was suggested also developed with VSCs (voltage source converters) that connect PV as well as battery resources with AC grid. To maximize the PV array's intermittent energy generation, a DC-DC buck converter as well as a maximum power point monitoring feature was used. For all grid-connected as well as island functioning approaches, a controller is recommended and used. In connected grid mode the grid regulates device's frequency as well as voltage. In isochronous phase, the fuel engine regulates the frequency as well as voltage of the system during an island mode fault. The suggested control proposal's efficacy was tested using effects from a real-time computer simulator.

3. Micro Grid Power Management System

A promising way to widely incorporate DER (distributed energy resource) systems is micro grids. regarded primarily a bracing technique together in smart grid design, micro grids provide potential power network solutions for both consumers and device operators. However, as a challenging task, prior literatures have not concentrated on the optimum administration as well as monitoring of many generations, loads, and storage resources localized in a micro grid. As a result, the MG is a very effective way of combining various DGs as well as energy storage systems in grid-linked or stand-alone function. ESDs (Energy storage devices) contribute a constitutive lead in stand-alone DC MG (micro grid) systems since they are used to equalize for power generation and load demand fluctuations. Furthermore, in a dc micro grid, the most critical factor in the micro grid power management scheme is to have excellent load voltage regulation even though input voltage from renewable sources varies greatly. The need for a massive duty ratio in order to contribute increased gain was a major drawback of traditional DC-DC boost converters. In addition, recent literatures addressed concerns including EMI (electromagnetic interference), reverse recovery, and low efficiency, among others. There continues to be a compelling need to create a controller that can demonstrate its suitability in a situation where the load and input voltage are both highly variable. During these conditions, efficient regulation of DC connection voltage at separate buses or several battery energy storage units is needed to eliminate power flow fluctuations as well as transients on the DC connection voltage.

DG (distributed generation) units have recently attracted a lot of attention because they deliver better performance, stability, and reliability than traditional power systems. As a result, the MG is a very effective way of combining various DGs as well as energy storage systems in grid-linked or stand-alone function. Though there is a huge lack of variations in load voltage, flow fluctuations and poor control of the DC connection with different bus voltages in the battery storage unit have been reported in prior literature. Hence this paper efficiently proposed the Tripartite Managed DC-DC convertor that highly reduces the load voltage variations in micro grid. A new kingpoint acolyte-based, distributed consonance management control is added to regulate the load-voltage in the micro grid as well as fluctuations of the input voltage by a combination with three variables of control (for example switching frequency, duty ratio, and phases change between two diligent connectors). In this way, active and passive control layers can be used to achieve the control objectives. The active stage uses a reference-oriented droop controlling technique to assign load components in batteries for voltage power.

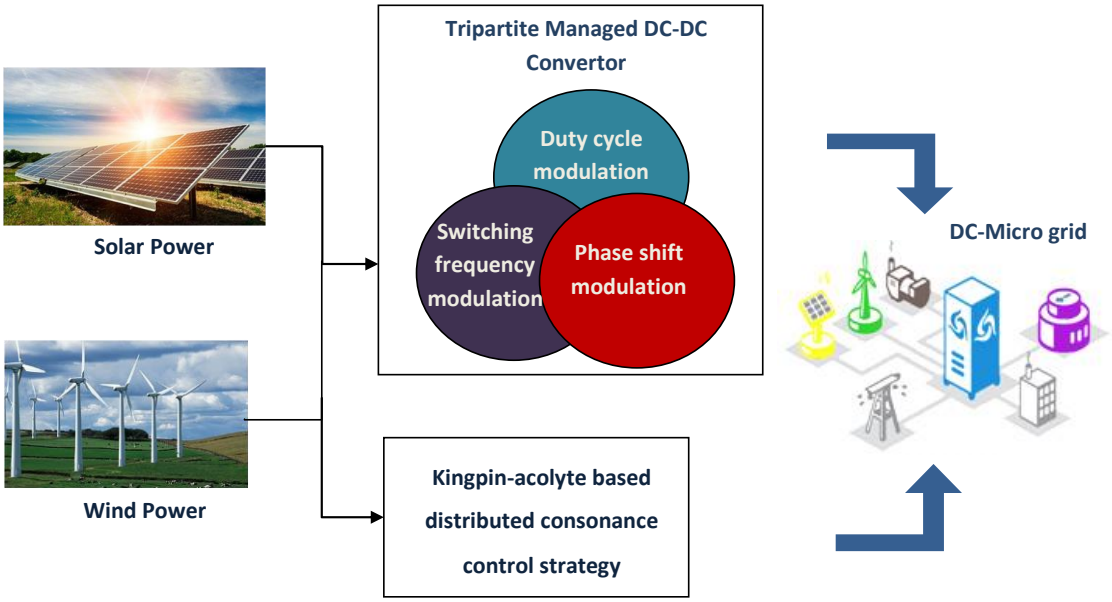

Fig. 1 Proposed block diagram.

To restore a stable DC bus voltage and ensure controlled power transfer among the battery energy storage devices, the passive layer employs a sequential multi-agent system-based distributed consensus. As a result, the proposed controller effectively and cost-effectively addresses the main significant issues in micro grid power management, such as load voltage inconsistencies, power flow volatility, and inadequate regulation of DC communication with separate bus voltage in battery storage unit. The following parts include more in-depth descriptions of these factors.

3.1 Tripartite Managed DC-DC Convertor

In order to build a DC control system for output voltage management in load and changing input voltage, three control variables gt, e, and ψ are utilized. The transition phase ψ12 is the difference between the input and output active bridges' square wave voltages. Two people have an effect on several factors. gt and e are used to constrain the result in terms of load, trying to keep the phase shift stable. Control variable ψ was utilized for getting the most power out of the output voltage in comparison to the input voltage while maintaining the switching frequency as well as duty time constant. Phase change ψ, represents deemed optimistic if Wbc performs Wb'c' and power is transferred from the source to the load. The output voltage is regulated by varying the switching frequency of standard switching frequency control. As a consequence, output voltage was sustained by adjusting the load ratio in cycle power.

The resonant frequency ω is described in below Equation (1),

$$\omega = \sqrt{\left[\left(\frac{1}{2M_1D_1}\right)\beta\left(\alpha+\sqrt{\alpha^2-4}\right)\right]} \tag{1}$$

where,

$$\beta = \sqrt{\frac{D_1}{D_2}\frac{M_1}{M_2}} \tag{2}$$

$$\alpha = \sqrt{\frac{D_1}{D_2}\frac{M_1}{M_2}} + \sqrt{\frac{D_1}{D_2}\frac{M_2}{M_1}} + \sqrt{\frac{D_2}{D_1}\frac{M_2}{M_1}} \tag{3}$$

$$A_{bd}\frac{8S'_M\cos\sigma}{\pi^2} = S_{bd}\cos\sigma \tag{4}$$

$$\sigma = \phi - \varphi_1 \tag{5}$$

$$A_q = \frac{-iA_{bd}}{\left(\omega_t D_q A_{bd} - i\right)} \tag{6}$$

$$A_t = \left(i\omega_t M_1 - \frac{i}{\omega_t D_1} \right) \tag{7}$$

$$A_{qq} = \frac{-i\omega_t M_2}{\left(\omega_t^2 D_2 M_2 - 1\right)} \tag{8}$$

$$A_{in} = A_q + A_t + A_{qq} \tag{9}$$

The switching frequency function, as expressed in, is the complete impedance of the Ain resonant tank (Equation (9)). The phase angle of Ain impedance is a function of frequency switching as well, and is calculated using Equation (10).

$$\varphi = h(\omega_t) = \tan^{-1}\left[\frac{\omega_t M_1 - \frac{1}{\omega_t D_1} - \frac{\omega_t M_2}{\omega_t^2 M_2 D_2 - 1} - \frac{\omega_t D_{qA_{bd}^2}}{1+\omega_t{}^2 D^2{}_{qA_{bd}^2}}}{\frac{A_{bd}}{1+\omega_t{}^2 D^2{}_{qA_{bd}^2}}} \right] \tag{10}$$

Since output terminal voltage rises under light loads and when input voltage is high, output voltage regulation requires a lower voltage gain. To ensure the highest output voltage, the proposed controller adjusts the duty ratio and frequency at the same time while maintaining the phase shift unchanged. Due to two control variables, the output voltage may be controlled with less frequency and duty cycle variation. The steady state performance is investigated using parabolic resonance frequency currents and voltages. wbc(u), which circulates current jL(u) in the tank circuit, can be used to measure the input voltage applied to the resonant tank network if the task ratio for all switches is Equation (11).

$$w_{BCbc}(u) = 2\sqrt{2}\,\frac{A_{in}}{\pi}\left[1-\cos(2\pi e)\right]^{1/2}\sin(\omega u + \psi) \tag{11}$$

The voltage step angle wbc(u), ψ is a job ratio d function that can be interpreted in the following way: Equation (12). Equation (13) describes the total voltage gain of the converter in terms of duty and frequency.

$$\psi = g(e) = \tan^{-1}\left[\frac{\sin(2\pi e)}{1-\cos(2\pi e)} \right] \tag{12}$$

$$N = \frac{U_{out}}{U_{in}} = \frac{2A_q}{o\pi A_{in}}\sqrt{1-\cos 2\pi e} = L_1 \frac{A_q}{A_{in}}\sin(\pi e) \tag{13}$$

$$L_1 = \frac{2\sqrt{2}}{o\pi} \tag{14}$$

The variance of the voltage gain of the converter, N with the normalized switching frequency, Z_t for maximum load and 30 percent rated load at various duty cycles. Duty cycle differences have a greater impact on lighter loads than on maximum loads.

The new frequency, g'T and duty cycles e' corresponding to changes in output voltage owing to load change are computed using the existing procedure (Equation (17)). If the U_O and U_{Oref} are the real voltages and the output voltages, the uD control, which is proportional to the downstream phase of the voltage may be measured using Equation (15).

$$u_D = l'\left(U_o - U_{oref}\right) \tag{15}$$

$$g_T' = g_T + u_D l_g \tag{16}$$

$$e' = e - u_d k_e \tag{17}$$

The value of the resonant current, jM1, sagging through the resonant network at any given time can be calculated using Equation (18).

$$\mathrm{j_{M1}}(u) = \frac{2\sqrt{2U_{in}}}{\pi A_{in}}\left[1-\cos 2\pi e\right]^{1/2}\sin(\omega u + \psi + \phi) \tag{18}$$

$$\delta = \phi - \psi > 0 \tag{19}$$

$$\phi > \psi$$

The various angles $\delta = i(\omega_t, e), \phi = h(\omega_t)$ and $\psi = g(e)$ are represented as a function of the control voltage, uD. The δ angle is greater than zero during the proposed approach over a wide range. As a result, ZVS (Zero Voltage Switching) is guaranteed if the renewed pace, and the renewed service period, e' are held within limits.

3.1.1 Renewable Sources Reduced Input Voltage Condition

As the input power is reduced while the converter is operating at maximum load, the converter's output voltage tends to be reduced as well. To achieve the necessary DC bus voltage output, increased converter gain is required.

(1) Essential of duty ratio:

That is very essential to note because if gain increases are needed, the duty ratio e' must be improved, but that is not possible as the limit at full load has already been set. Lowering the switching frequency will also improve the gain as the resonant frequency is already set at maximum load. The gentle switching will be deactivated if the switching frequency is decreased below the resonance frequencies. The triple control signal 12 is also utilized under the same conditions to amplify signals so that the input voltage from RES (Renewable Energy Source) is reduced. The angle φ_{12} represents phase change among input and output square wave voltages.

The phase shift ψ12 is considered optimistic if UB'C' lags UBC. A two-port active converter with either a load-side active bridge or a load-side diode rectifier bridge is said to have a slightly higher voltage gain. The phase difference between two converter ports will range from 00 to 900. Unless the maximum power is RL, the transformer turns ratio represented as n, as well as the load current represented as Jo, the output voltage Uo = JoRL can be expressed using phase shift ψ12 (Equation (20)),

$$N_2 = \frac{o}{n}\sin(\phi_{12}) \tag{20}$$

$$n = Q\left(Z_T - \frac{1}{Z_T}\right) \tag{21}$$

$$Z_T = \frac{\omega_T}{\omega_p} \tag{22}$$

$$Q = \frac{\omega_p M_1}{R'_M} \tag{23}$$

The phase shift angle, φ_{12}, is calibrated to be positive for active power from Port 1 to Port 2. As a result, output voltage increases while the phase difference among activated bridges rises.

(2) ZVS condition at the time of control:

If Port 1 is new, UBC, the zero voltage switching of entire switches in Port 1 bridge, then jM1 has its applied square wave voltage lagging due to the soft switch-condition in active bridges. However, the ZVS specification for Bridge 2 specifies that if Port 2 poses UB'C', after every switches with in Port 2 bridge will flip to zero voltage. The recommended control approach checks also meet those requirements.

$$\phi'_{12} = \phi_{12} + l_q * u \tag{24}$$

$$u = l_1(u_{inref} - u_{in}) \tag{25}$$

Based on a change in renewable source input voltage, the proposed algorithm calculates the necessary renewed phase shift, φ'12 (Equation (24)). If Uin and Uinref are the input voltage real reference as well as input voltage, correspondingly, then u (Equation (25)), with l1 as a scaling factor to reduce the voltage to the DSP tolerable level, can be used to measure the actuating control voltage. lq is a phase change constant.

In the proposed control unit, an appropriate control system is very important for efficient power management and soft switching service. The U0 output grid DC is controlled by using the gT, duty ratio e' and external phases shift φ'12, as indicated in Equation (14) and as a

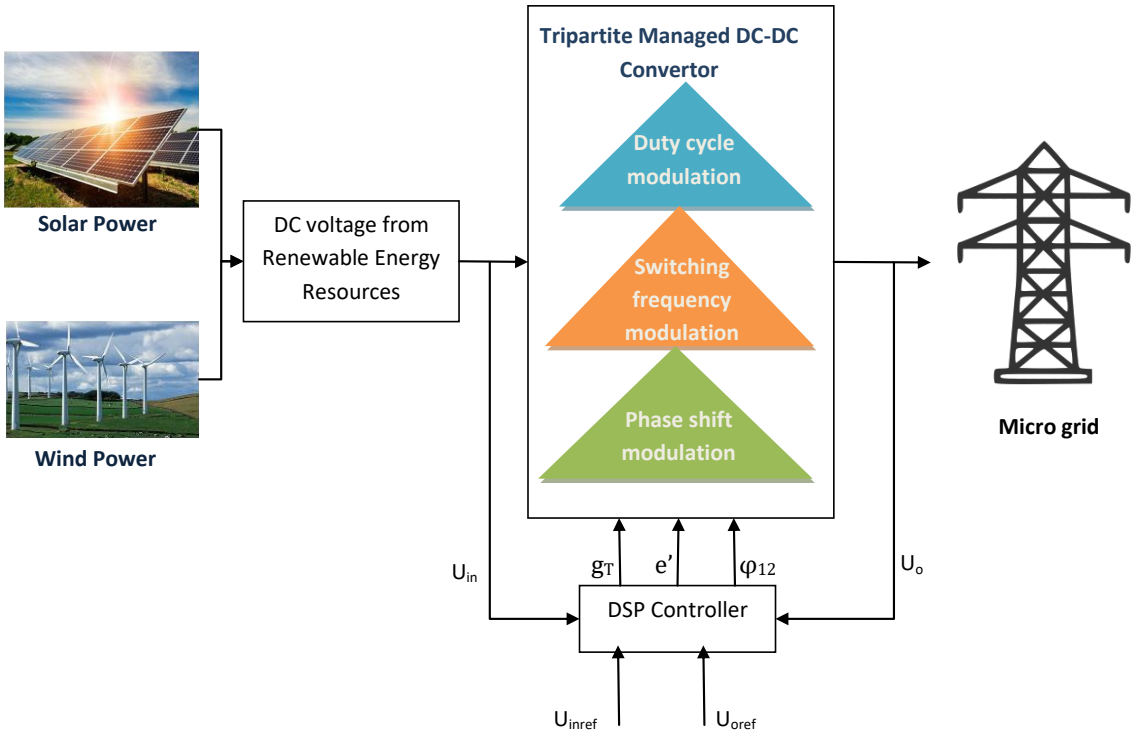

Fig. 2 Architecture of proposed converter.

control variable (Equation (20)). As a result, the output voltage can be modified with different gT; d varies with regard to DC load changes and φ12 in relation to input voltage variations. Fig. 2 depicts a suggested converter's closed loop controlling architecture. By comparing the voltage U0 to the reference signal, an incorrect signal is obtained. A compensator, also called a digital controller, transmits the error signal to the modulator and transmits an actuating signal. The modulator produces a switching sequence having its required switching frequency, duty ratio, appropriate external phase shift, afterwards transfers the battery energy from the storage unit to the driver circuit.

3.2 Kingpin-Acolyte Based Distributed Consonance Control Strategy

In this kingpin-acolyte based distributed consonance control strategy incorporates five battery units, which are composed through the MG system, whereas each Battery Energy Storage Unit is an agent. In this work, the idea of MRS (Multi Representative System) is used to set up the protocol for consonance control. Each BESU (Battery Energy Storage Unit) communicates with its neighbours in order to maintain a healthy energy level and share power around the ESUs (Energy Storage Units). Using sparse communication graphs, the required communication network can be created. Next, a brief introduction to the theory of graphs is given. The DC bus voltage for the battery unit is then controlled by the cooperative secondary voltage controller. Finally, the requirements for implementing secondary voltage regulation in communication networks are discussed.

3.2.1 Kingpin-Acolyte Secondary Voltage Control

The MRS computer distinguishes five battery units in order to accomplish the main control goals and function autonomously with limited contact. The Battery Kindpin and four Battery Followers are the five MRS machines. All of the BESUs interact with each other via a small communication network referred to in letter H. The data yj is received by the battery follower device straight from leading battery module y0, because of a so-called weight factor called pinning gain hj, and only one BESU access the reference y0. Each BESU should

translate information yi over a communication network to its neighbor in accordance with digit H.

As shown in Fig. 3, the leader is supplied to offset the voltage divergence caused by the reduction in power. A PI control picture is used to compute P_{King}, which is a battery power signal employed to regulate the leader battery voltage and the overall DC bus voltage of the microgrid. These are the leading representative equations for control.

$$P_{King} = PI_K(u_{MG} - u_{Bat}) \tag{26}$$

$$PI_K l_{KingP} + \frac{l_{KingI}}{t} \tag{27}$$

$$u^* = u_{MG} - s_j\left(P_{Bat} - P_{King}\right) \tag{28}$$

The gains of the chief voltage controller are lKingP and lKingI. The battery follower modifies the droop voltage output by instigating the power signal P^*_{coop} using a cooperative control design as seen in Fig. 3.

$$u^* = u_{MG} - s_j(P_{Bat} - P^*_{Coop}) \tag{29}$$

$$P^*_{Coop} = u_{MG} - (PI_u F\bar{u}_j + PI_{ToC} F\bar{T}oC_j) \tag{30}$$

Therefore, P^*_{coop} is controlled by changed voltage control and load balancing fault signal monitoring status. Finally, in Equation (34) to rearrange the voltage change, the Voltage Correction signal is given:

$$F\bar{u}_j = b_{jk}(\bar{u}_k - \bar{u}_j) + h_j(\bar{u}_0 - \bar{u}_j) \tag{31}$$

$$F\bar{T}oC_j = b_{jk}\left(\bar{T}oC_k - \bar{T}oC_j\right) + h_j\left(\bar{T}oCo - \bar{T}oC_j\right) \tag{32}$$

$$PI_u = l\bar{u}P + \frac{l\bar{u}I}{t}, PI_F = l_{ToCP} + \frac{l_{SoCI}}{t} \tag{33}$$

$$\bar{u}_j(t) = u_j(t) + \int_0^t \sum_{k\in O_j} b_{jk}\left(\bar{u}_k(t) - \bar{u}_j(t)\right)dt \tag{34}$$

where, $l\bar{u}P$ and $l\bar{u}I$ were the control gains of improved voltage controller, l_{ToCP} and k_{ToCI} were the control gains of ToC regulation loop, $F\bar{u}_j$ and $F\bar{T}oC_j$ were the neighborhood modified voltage tracking error also ToC tracking error of each battery.

3.2.2 Design of Control Input

The bulk of MAS's (Multi-Agent System) battery control distributed consensus control architecture is centered on precise control or Lyapunov design. The Lyapunov design discussed in this section. A complicated model of a battery chief is as follows:

$$\dot{y}_0 = By_0 \tag{35}$$

where, $y_0 \in S^m$ represents the battery leader state. $y_0 \rightarrow u_{MG}$ represents the battery leader should track u_{MG}.

The following equation describes the i^{th} follower's energy storage module's characteristics as follows:

$$\dot{y}_j = By_j + Cv_j, j \in O \tag{36}$$

where, $y_j \in \Re^m$ represents battery state vector; the leader voltage must be synchronized by battery follower. $y_i \rightarrow y_0$ and $v_j \in \Re^n$ represent i^{th} battery follower's control input. B as well as C represents the system's state matrices; also (B, C) was considered as stable.

Furthermore, secondary voltage controllers are expected to restore the voltage in stand-alone mode fast to its nominal value. In this investigation, this design is made simplified by the dynamics of inner voltage as well as current controllers. It is possible to write the dynamic of each BESU accordingly:

$$\begin{bmatrix} \dot{\Delta}F_j \\ \dot{\Delta}U_j \end{bmatrix} = \begin{bmatrix} 0 & 1 \\ 0 & 0 \end{bmatrix} + \begin{bmatrix} F_j \\ U_j \end{bmatrix} \begin{bmatrix} 0 \\ 1 \end{bmatrix} + v_j \tag{37}$$

where,

$$y_j = \begin{bmatrix} y_j y_j, & 1 \end{bmatrix}^T \quad B = \begin{bmatrix} 0 & 1 \\ 0 & 0 \end{bmatrix}, C = \begin{bmatrix} 0 & 1 \end{bmatrix}^S$$

B and C are the system's state matrices, and each battery's energy and voltage are F_j and U_j.

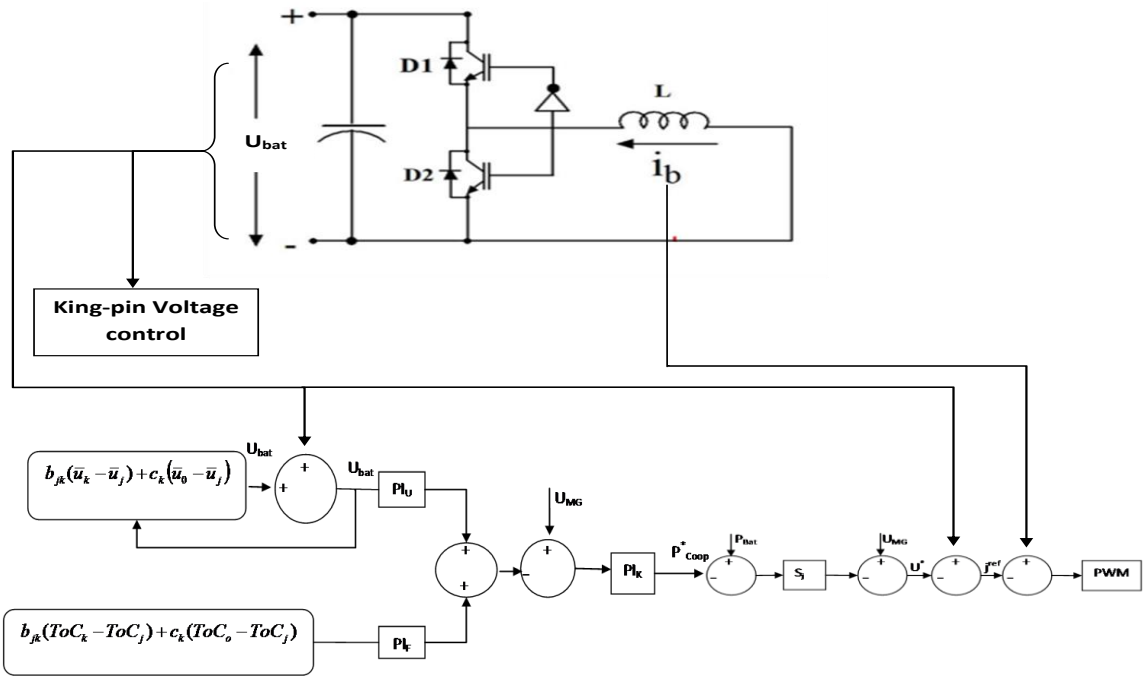

Fig. 3 Proposed kingpin-acolyte based distributed consonance controller.

The vj consensus protocol must be used to synchronise the terminal voltage (uj) and state of charge (ToCj) of each battery cell with the reference voltage (u0) for secondary voltage regulation (Equation (16)). Local group monitoring mistake (Equation (10)) & members of the cooperative management committee are expressed in the form of Equation (11). The voltage difference between neighbours can be used to regulate DC connection voltage by sending it as a control input to each BESU. Fig. 3 depicts the configuration of a V-P-based leader-follower voltage controller.

The designed controller consists of primary as well as secondary control levels, as shown in Fig. 3. And that is responsible for the control of voltage. By tuning PI controllers, larger transients can be minimized.

$$v_j = dL\left[\sum_{i=1}^{M} b_{jk}(y_k - y_j) + h_j(y_0 - y_j)\right] \quad (38)$$

To choose the right control gain L, the LQR (linear quadratic regulator) approach was utilized. The controller input gain L in Equation (39) could be designed as follows since the Q and S matrices are all positive definite:

$$L = S^{-1}C^U P \quad (39)$$

P is the algebraic Riccati equation's special positive definite solution (ARE). The algebraic Riccati equation parameters S and Q have a direct impact on the controller's transient reaction.

3.2.3 Stability Control

Closed-loop structures must be addressed when evaluating the proposed control scheme's stability. The addition of the control input defined Equation (40) to the system approach leads to:

$$\dot{y}_j = By_j + C\left(dE\left[\sum_{i=1}^{M} b_{jk}(y_k - y_j) + h_j(y_0 - y_j)\right] - D_{0j\hat{\bar{y}}}\right) \quad (40)$$

where, j ∈ M where λmin = min{Re(λ) : λ ∈ σ (H)}.

The entire closed-loop structure on a global scale can be described as:

$$\dot{y} = B_d y + C_d \underset{-0}{y} + \overline{C}\overline{D}_{of} \quad (41)$$

The letter i is used to represent the individual values of the Laplacian matrix L graph. The stability characteristics of Equation (42) result from the global system dynamics stability requirements:

$$\dot{a}_j = (B - \lambda_j dCL)a_j \quad (42)$$

The stability criterion necessitates $\dot{a}_j = (B - \lambda_j dCL)a_j$; all of its own ideals have to be purely negative or to be Hurwitz's real component. To select the coupling gain d, an adequate condition is needed as:

$$d \geq \frac{1}{2\lambda_{\min}} \tag{43}$$

From the above-mentioned concerns clearly denote that the proposed convertor and control strategy tackles the major obstacles such as decreases the variations in load voltage, power flow fluctuations, and enhanced the control of DC connection with different bus voltage in battery storage units. Hence those are tackled through novel Tripartite Managed DC-DC convertor that highly reduces the load voltage variations in micro grid, which performs through switching frequency, duty ratio, as well as phase shift among 2 active connectors. Along with this the research work introduces the kingpin-acolyte based distributed consonance control strategy for ensuring the balanced power flow and enhanced the battery storage unit control. The next section elaborately and virtually demonstrates the outcome of the proposed work in an effectual manner.

4. Result and Discussion

This section elaborately described the competence of the proposed analysis of numerical simulation of the novel converter and battery energy storage control strategy developed in previous section.

4.1 System Specification

The following table defined the system specifications, which is used in the proposed work to evaluate the competence of the research.

Table 1 Simulation environment specifications.

Platform	MATLAB 2017b
OS	Windows 8
Processor	Intel core i7
RAM	8 GB

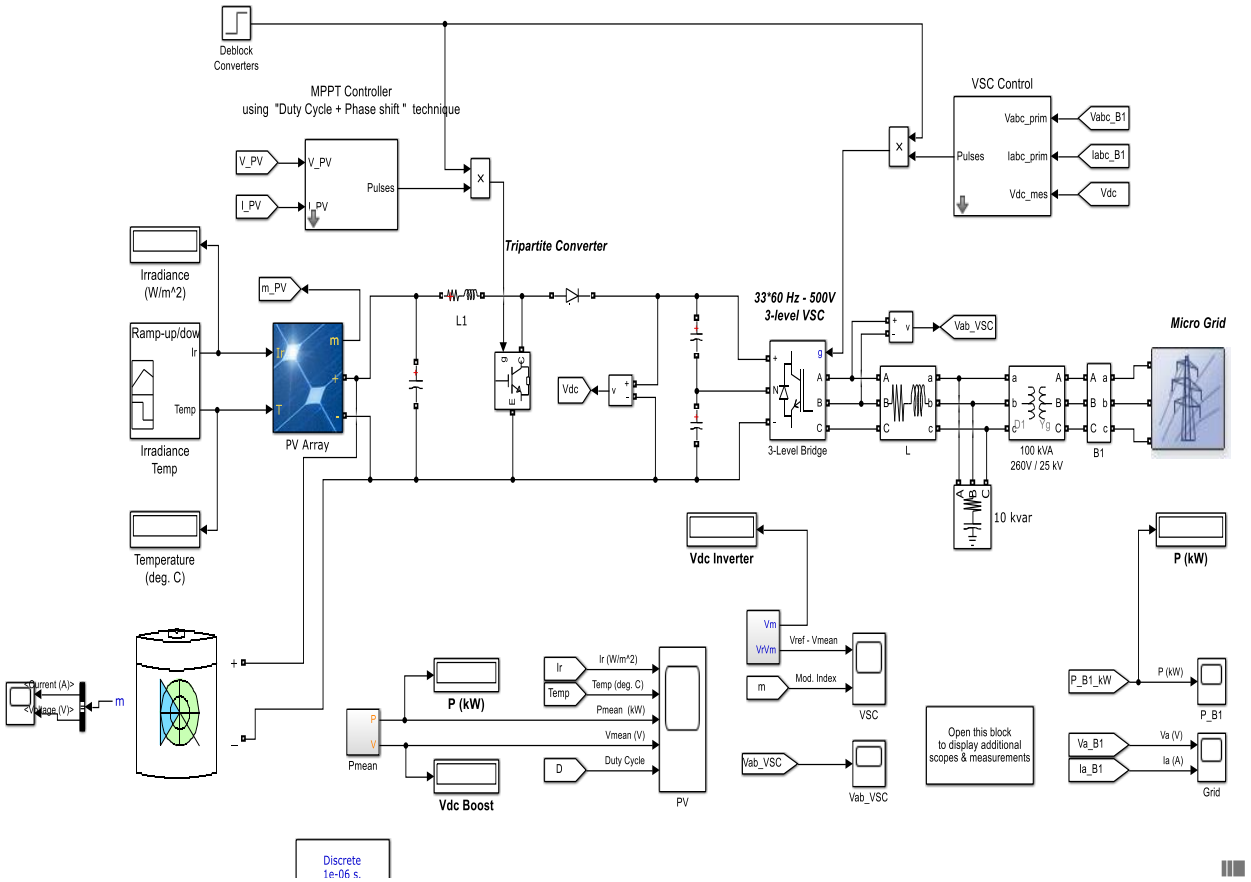

Fig. 4 Simulation model.

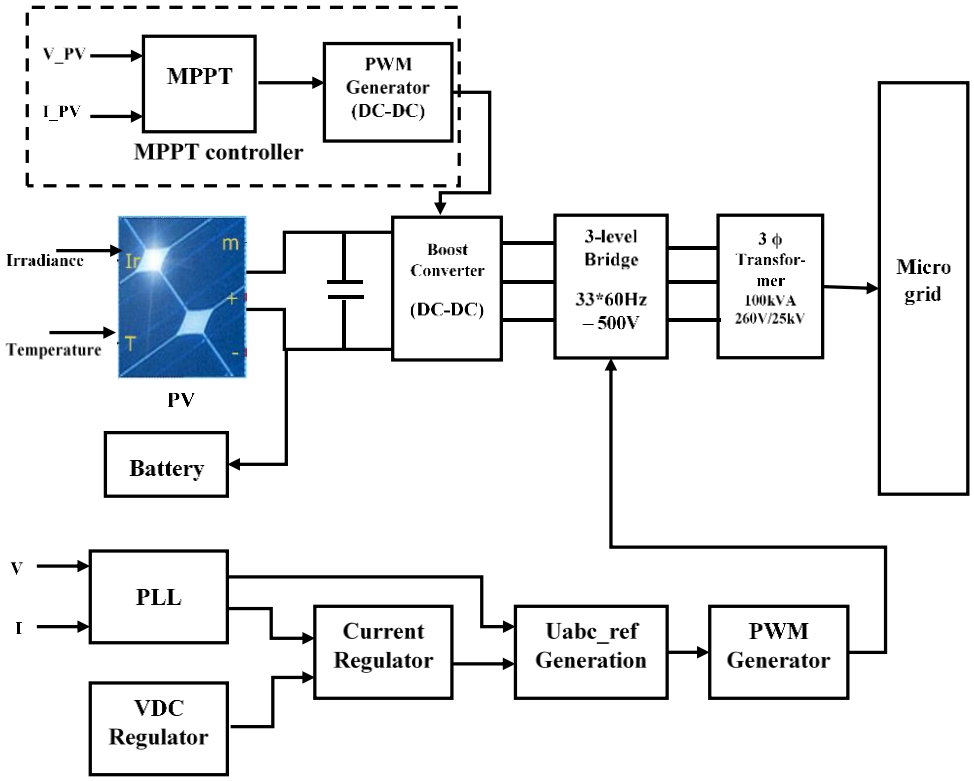

Fig. 5 Block diagram of the simulation model.

Table 2 Input system specifications.

Si. No.	Specifications	Range
1.	Voltage input range	260 V-180 V
2.	Specified input voltage	220 V
3.	Specified output voltage	400 V
4.	P_o	3,000 Watts
5.	Resonant frequency	100 kHz
6.	Series tank parameters	L1 = 52.12, C1 = 56.23 nF
7.	Parallel tank parameters	L2 = 521.2, C2 = 562.3 nF
8.	Parallel capacitor	C_P = 5.432 nF, $C'_P = n^2C_P$ = 1.654 nF
9.	Capacitor filter	0.3 nF
10.	Ultra-fast switches, IGBTs	30N60A4D
11.	HF Transformer	Ferrite core PM 62, n = 0.55

4.2 Simulation Analysis

Figure described the simulation design of the proposed model, that outperformed the enhanced power quality conversion framework and battery energy storage control strtaegy. The converter has been investigated experimentally with varied load as well as various input voltages that evaluate the functioning of a proposed control.

The dynamic output is evaluated and shown in the following section with phase changes in supply voltage.

Fig. 6 described the variation of pressure, temperature, voltage and duty cycles that is based on particular time period. Here the time period is varied from 0 to 2.5; here temeperature is rised from 25 to 50 inbetween the time period of 2 to 2.15. Power variations are stabilized at the point of 95 kW between 2 to 2.5. Hence it elaborately described the performance of the converter that highly reduces the load voltage variations.

When the system is under PQ control mode in the V/F control mode, the voltage reference level equals its recorded amplitude and the phase angle is where the recording phase angle is when the storage device was operating in PQ mode, following the storage system's transition to V/F mode of operation. Thus the reference voltage and their mean value with modulation index are illustrated in Fig. 7.

The DC connecting voltage and charge (SC) reaction is shown in Fig. 8. The charging mechanism of the MG system and the synchronization of power with load changes by the ESUs is shown in Fig. 9. The DC connection voltage fluctuates when the load changes.

Voltage and current variations are the frequency which is at its lowest value and its highest value is the service period. The proposed regulation's main concern is converter performance, whenever the input voltage gets decreased during rated load. The input voltage is progressively lowered from the stated value. Whenever the input voltage gets lowered, the phase shift increases, and the DC output voltage was regulated, as shown in Fig. 10.

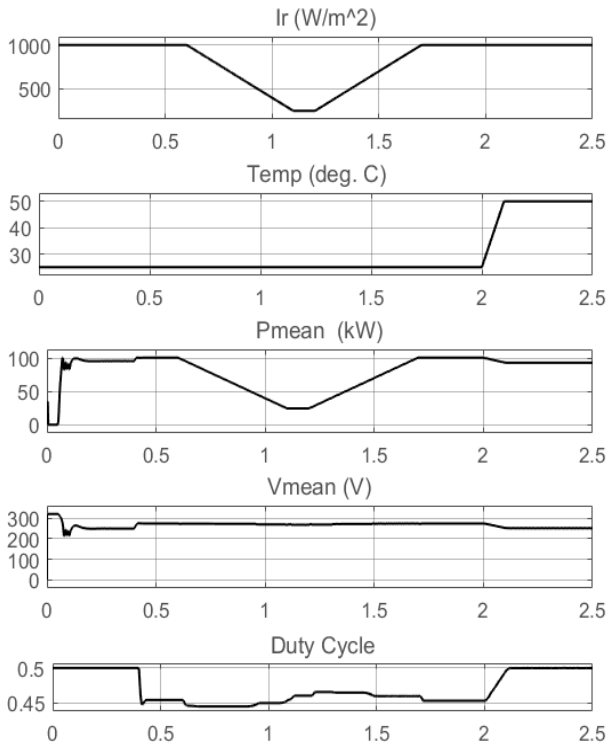

Fig. 6 Proposed variations ranges.

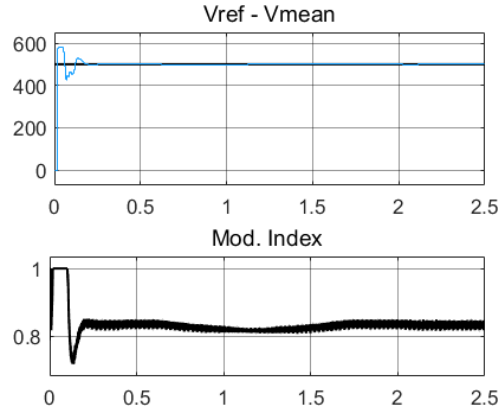

Fig. 7 Reference voltage based on mean and modulation index.

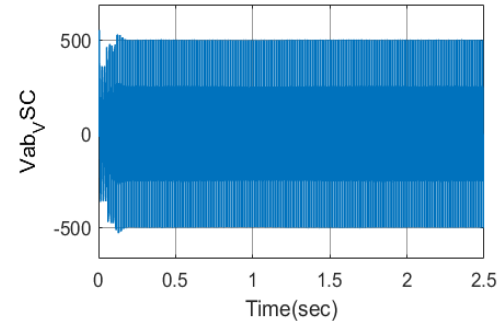

Fig. 8 DC link voltage and SC responses.

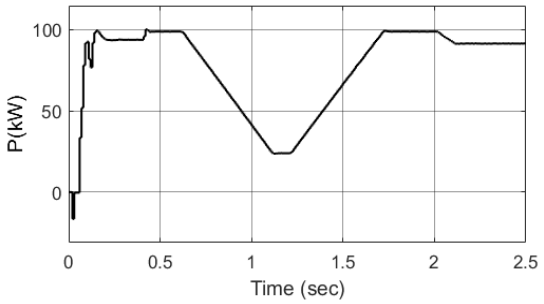

Fig. 9 Power as per the change in load.

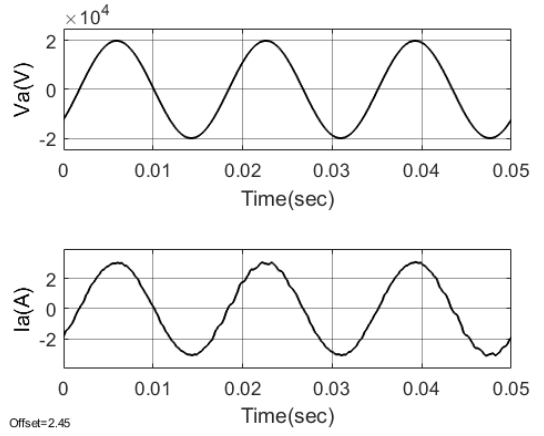

Fig. 10 Regulation of DC output voltage.

Thus the Fig. 11 depicted proposed strategy control of current and voltage in the battery storage unit within fraction of seconds. Here at certain point of time as 2.5 second current is reached at 1,500 amps and voltage 229 V.

4.3 Comparison Analysis

Fig. 12 shows the power supply in a micro grid system of one of the two mixed electricity storage subsystems. The SoC for the two integrated energy storage subsystems pre-set is shown in Fig. 12 to be 0.75 and 0.25, each. The output ratio of the two should be 3:1 and 1:3 in the discharge and charge state, according to the proposed Solution Strategy. For 0.5-1 s, the two subsystems generate 570 as well as 190 W, correspondingly. For 2-3 seconds, the two subsystems produce 215 as well as 645 W, respectively, which is consistent with theory. The feasibility of the hybrid energy storage subsystem power distribution approach centered on SOC was competently established.

Fig. 13 illustrates the comparison of different components with various topologies. The figure shows that the proposed strategy efficiently achieves reduced component counts, with only 3 active switches, 6 diodes, 2 magnetic cores, 5 windings, and 3 capacitors. From this comparison, it is evident that the proposed controller and converter design requires a minimal and efficient amount of hardware to regulate load voltage variations and improve power flow, ensuring effective energy control in the battery energy storage system.

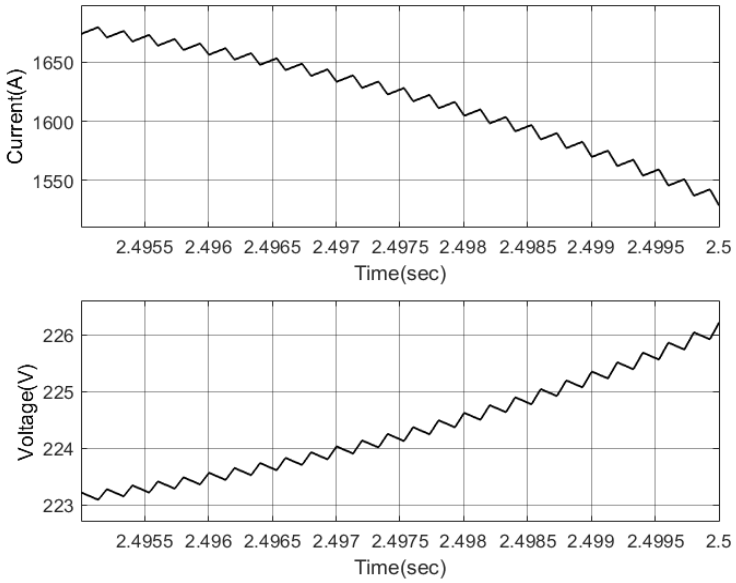

Fig. 11 Control of current and voltage in battery storage unit.

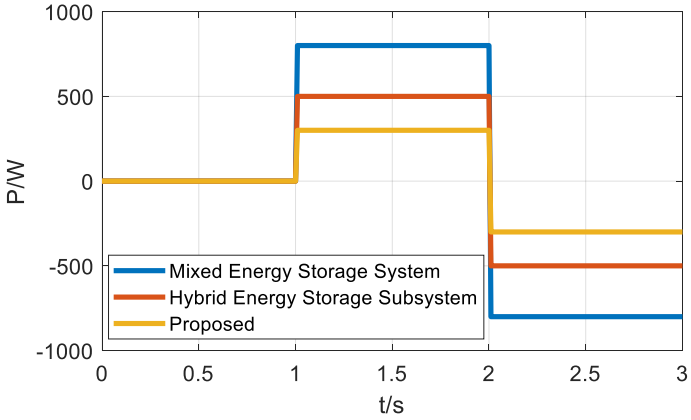

Fig. 12 Comparison analysis of power distribution of a subsystem in a micro grid.

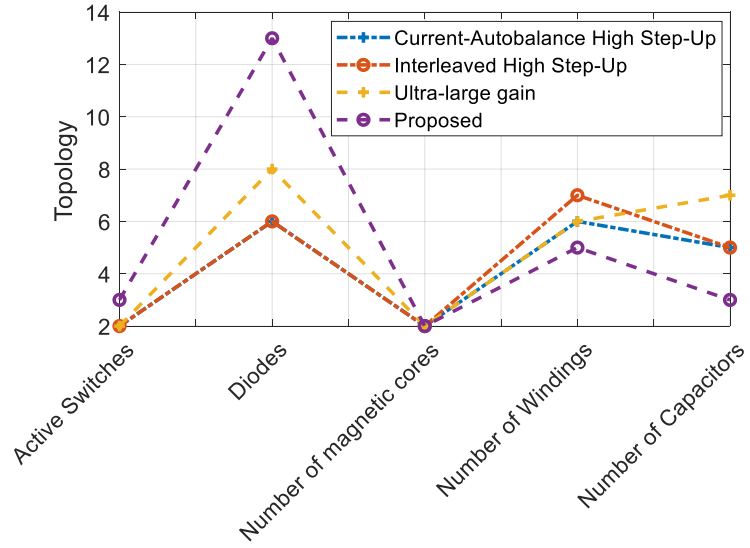

Fig. 13 Comparison of different components with variant topologies.

5. Conclusion

In this paper, a Tripartite Controlled DC-DC Converter with three control variables for a changed series parallel resonant tank converter is suggested to connect renewable sources to a microgrid's DC bus. This controller has excellent ZVS, enhanced reliability, and voltage regulation for the reduction in the input voltage under full load from renewable sources. A distributed consonance control method is also being employed to build a secondary tensile control system for the battery unit to restore the DC bus voltage based on kingpins and acolytes. The DC-follower V-P control provides superior DC voltage management with a minor deviation and an appropriate power balance between sources in comparison with a leaderless controller.

Authors' contributions: All authors equally contributed in this work.

Data availability: The data is available with the authors.

Code availability: The custom MATLAB code is available with authors.

Declarations

Conflict of interest/Competing interests: On behalf of all authors, the corresponding author states that there is no conflict of interest.

References

[1] Brazier, F., Poutre, H. L., Abhyankar, A. R., Saxena, K., Singh, S. N., and Tomar, K. K. 2015. "A Review of Multi Agent Based Decentralised Energy Management Issues." In *International Conference on Energy Economics and Environment (ICEEE)*, pp. 1-5. Noida, India.

[2] Singh Tomar, K. K., and Singh, S. N. 2016. "Energy Management and Control of Microgrid Using Multi-Agent Systems." In *UP Section Conference on Electrical Computer and Electronics*, pp. 1-6.

[3] Singh Tomar, K. K., and Singh, S. N. 2017. "An Agent-Based Approach for Efficient Energy Management of Microgrids." In *IEEE Region 10 Symposium (TENSYMP)*, pp. 1-5.

[4] Singh Tomar, K. K., and Singh, S. N. 2021. "Level-One House Agent-Based Decentralized Resilient Energy Management." On SCI Indexed Journal *Springer Nature Electrical Engineering*, 1-9.

[5] Singh Tomar, K. K., and Singh, S. N. January 2025. "Multi-Agent System Based Active Power Management in Micro-Grid." *International journal of Innovative Research in Technology* 11 (8). ISSN:2349-6002.

[6] Cheng, Z., Li, Z., Li, S., Gao, J., Si, J., Das, H. S., and Dong, W. 2020. "A Novel Cascaded Control to Improve Stability and Inertia of Parallel Buck-Boost Converters in DC Microgrid." *International Journal of Electrical Power & Energy Systems* 119: 105950.

[7] Zhang, Q., Zhuang, X., Liu, Y., Wang, C., and Guo, H. 2020. "A Novel Control Strategy for Mode Seamless Switching of PV Converter in DC Microgrid Based on Double Integral Sliding Mode Control." *ISA Transactions* 100: 469-80.

[8] Ma, W., and Ouyang, S. 2019. "Control Strategy for Inverters in Microgrid Based on Repetitive and State Feedback Control." *International Journal of Electrical Power & Energy Systems* 111: 447-58.

[9] Liu, Y., Guan, L., Guo, F., Zheng, J., Chen, J., Liu, C., and Guerrero, J. M. 2019. "A Reactive Power-Voltage Control Strategy of an AC Microgrid Based on Adaptive Virtual Impedance." *Energies* 12 (16): 3057.

[10] Mohammadi, J., and Ajaei, F. B. 2019. "Improved Mode-Adaptive Droop Control Strategy for the DC Microgrid." *IEEE Access* 7: 86421-35.

[11] Menniti, D., Pinnarelli, A., Sorrentino, N., Vizza, P., and Barone, G. 2019, June. "A Community Microgrid Control Strategy to Deliver Balancing Services." In *2019 IEEE Milan PowerTech*, pp. 1-6. IEEE.

[12] Mi, Y., Chen, X., Ji, H., Ji, L., Fu, Y., Wang, C., and Wang, J. 2019. "The Coordinated Control Strategy for Isolated DC Microgrid Based on Adaptive Storage Adjustment without Communication." *Applied Energy* 252: 113465.

[13] Jiao, J., Meng, R., Guan, Z., Ren, C., Wang, L., and Zhang, B. 2019, June. "Grid-Connected Control Strategy for Bidirectional AC-DC Interlinking Converter in AC-DC Hybrid Microgrid." In *2019 IEEE 10th International Symposium on Power Electronics for Distributed Generation Systems (PEDG)*, pp. 341-5. IEEE.

[14] Peng, Z., Wang, J., Bi, D., Wen, Y., Dai, Y., Yin, X., and Shen, Z. J. 2019. "Droop Control Strategy Incorporating Coupling Compensation and Virtual Impedance for Microgrid Application." *IEEE Transactions on Energy Conversion* 34 (1): 277-91.

[15] Keshavarzi, M. D., and Ali, M. H. 2019, February. "FRT Capability Enhancement of Autonomous AC/DC Hybrid Microgrid by Coordinated MSDBR and Interlinking Converter Control Strategy." In *2019 IEEE Power & Energy Society Innovative Smart Grid Technologies Conference (ISGT)*, pp. 1-5. IEEE.

[16] Aboushal, M. A., and Moustafa, M. M. Z. 2019. "A New Unified Control Strategy for Inverter-Based Micro-Grid Using Hybrid Droop Scheme." *Alexandria Engineering Journal* 58 (4): 1229-45.

[17] Peng, Z., Wang, J., Wen, Y., Bi, D., Dai, Y., and Ning, Y. 2019. "Virtual Synchronous Generator Control Strategy Incorporating Improved Governor Control and Coupling Compensation for AC Microgrid." *IET Power Electronics* 12 (6): 1455-61.

[18] Naji Alhasnawi, B., Jasim, B. H., and Esteban, M. D. 2020. "A New Robust Energy Management and Control Strategy for a Hybrid Microgrid System Based on Green Energy." *Sustainability* 12 (14): 5724.

[19] Amirkhan, S., Radmehr, M., Rezanejad, M., and Khormali, S. 2020. "A Robust Control Technique for Stable Operation of a DC/AC Hybrid Microgrid under Parameters and Loads Variations." *International Journal of Electrical Power & Energy Systems* 117: 105659.

[20] Sedaghati, R., and Shakarami, M. R. 2019. "A Novel Control Strategy and Power Management of Hybrid PV/FC/SC/Battery Renewable Power System-Based Grid-Connected Microgrid." *Sustainable Cities and Society* 44: 830-43.

[21] Mehrasa, M., Sharifzadeh, M., Babaie, M., and Al-Haddad, K. 2020, June. "Power Sharing Management of a PEC9-Based Microgrid by Feedback-Feedforward Control Strategy." In *2020 IEEE 29th International Symposium on Industrial Electronics (ISIE)*, pp. 1062-7. IEEE.

[22] Wu, T., Ye, F., Su, Y., Wang, Y., and Riffat, S. 2020. "Coordinated Control Strategy of DC Microgrid with Hybrid Energy Storage System to Smooth Power Output Fluctuation." *International Journal of Low-Carbon Technologies* 15 (1): 46-54.

[23] Tummuru, N. R., Manandhar, U., Ukil, A., Gooi, H. B., Kollimalla, S. K., and Naidu, S. 2019. "Control Strategy for AC-DC Microgrid with Hybrid Energy Storage under Different Operating Modes." *International Journal of Electrical Power & Energy Systems* 104: 807-16.

[24] Toghani Holari, Y., Taher, S. A., and Mehrasa, M. 2020. "Distributed Energy Storage System-Based Nonlinear Control Strategy for Hybrid Microgrid Power Management Included Wind/PV Units in Grid-Connected Operation." *International Transactions on Electrical Energy Systems* 30 (2): e12237.

[25] Worku, M. Y., Hassan, M. A., and Abido, M. A. 2019. "Real Time Energy Management and Control of Renewable Energy Based Microgrid in Grid Connected and Island Modes." *Energies* 12 (2): 276.